Journal of Applied Polymer Science

WILEY

Applied Polymer SCIENCE

RESEARCH ARTICLE OPEN ACCESS

Use of Electrospun Cellulose Acetate/Silica Composites as Multifunctional Ingredients in Eco-Friendly Semisolid Lubricant Formulations

Manuel Toro-Gallego | Concepción Valencia | M. Carmen Sánchez | José E. Martín-Alfonso | José M. Franco

Department of Chemical Engineering and Materials Science, Pro2TecS – Chemical Product and Process Technology Research Center, Universidad de Huelva, ETSI, Campus de "El Carmen", Huelva, Spain

Correspondence: José M. Franco (franco@uhu.es)

Received: 27 June 2024 | **Revised:** 28 September 2024 | **Accepted:** 23 October 2024

Funding: This work was supported by Ministerio de Ciencia, Innovación y Universidades and ERDF/EU (PID2021-125637OB-I00).

Keywords: biopolymers and renewable polymers | composites | fibers | friction | nanostructured polymers | wear and lubrication

ABSTRACT

Cellulose acetate/silica (CA/SIL) nanocomposites are prepared by electrospinning and investigated as multifunctional ingredients in eco-friendly semisolid lubricant formulations. The structuring ability of these electrospun composites in castor oil and the antifriction and antiwear properties are examined through rheological and tribological experiments. The multifunctionality of CA/SIL composites arises from a balance between the silica content and the formation of nanofiber-dominated structures. The linear viscoelasticity functions in the oleo-dispersions increase by several orders of magnitude with both the spinning solution concentration and the CA:SIL ratio. However, the rheological response primarily depends on the morphology of the nanofiber mat obtained, specifically nanofiber diameter and the presence of beads. In contrast, the silica content significantly impacts the tribological performance of the oleo-dispersions regardless of nanofiber morphology. For similar nanoarchitectures and rheological responses, the friction coefficient is reduced from 0.227 to 0.108 by incorporating silica in a 10:1 CA:SIL ratio, compared with the SIL-free electrospun CA nanofibers, while wear is completely prevented. Increasing the composite concentration from 5 to 12.5 wt. % enhances wear protection and the gel strength of oleo-dispersions, for example, the plateau modulus rises from 800 to 42,000 Pa using a composite with a 10:1 CA:SIL ratio.

1 | Introduction

As the global economy and industrial activity rapidly develop, energy losses and machinery degradation caused by friction and wear are becoming increasingly significant in terms of profitability and energy savings. According to available statistical data, friction accounts for approximately 30% of the world's primary energy consumption, while wear leads to the failure of about 80% of mechanical components in machinery [1]. To address this issue, reducing friction and wear has become a key research focus in surface science and mechanical engineering [2]. Over the past decades, substantial advancements have been made in developing sophisticated lubricant formulations and additives designed for challenging and harsh working conditions, enhancing technical functionalities, and meeting increasingly stringent environmental requirements [3].

Lubricants are available in liquid, solid, semisolid, and gaseous states, with liquid and semisolid lubricants (lubricating greases) being the most commonly used in daily life. Commercial lubricants for industrial applications are complex fluids comprising base oil blends, a viscosity modifier or thickening agent (especially relevant for lubricating greases), and packages of functional additives. These additives include rheology modifiers,

friction reducers, anti-wear agents, extreme pressure additives, antioxidants, and pour point depressants, among others [4, 5] to improve energy efficiency and increase the service life of machine elements [6].

In recent years, the development of new and advanced lubricants has been increasingly driven by environmental awareness and pollution concerns. Consequently, there is significant interest in replacing traditional lubricant ingredients with biodegradable and/or naturally derived alternatives that maintain technical performance while mitigating environmental impact [7–10]. In this context, oil thickeners and rheology modifiers derived from natural resources (e.g., biopolymers or their derivatives) are emerging as environmentally friendly alternatives to traditional metallic soaps and synthetic polymers produced by the petrochemical industry. Previous studies have reported the development of eco-friendly oleogels using sustainable polymeric gelling or thickening agents from natural resources for vegetable oil media [11–17]. This requires improving the compatibilization between natural polymers and the oil medium, which can be achieved by reducing polymer polarity (e.g., by inserting nonpolar groups) or by functionalizing the biopolymer with reactive groups that form covalent bonds with triglycerides, promoting cross-linking between the vegetable oil and the polymeric thickener. However, these strategies often require complex chemical modifications, limiting the ecological added value of the entire production process. Recently, a novel approach involving electrospun biopolymer nanofibers for structuring vegetable oils has been introduced [18–21]. Due to their small size and high aspect ratio, suitably dispersed nanofibers promote oil structuring by forming a percolation network.

Electrospun natural polymers are widely used in environmental and medical applications due to their green, renewable, and degradable properties. These polymers can produce single-component nanofibers or multicomponent nanofibers incorporating metal oxides, silica, or clays to provide specific functionalities or alter the physicochemical properties of the spinning solution [22]. Generally, composites of cellulose or its derivatives and silica are prepared to combine the distinct properties of each constituent (e.g., mechanical, thermal, and sorption properties, vapor permeability, antimicrobial activity) and enhance processability [23–25]. The hydrophobic/oleophilic character of cellulose-based aerogels was balanced by incorporating modified silica nanoparticles [26]. The preparation of clay and cellulose derivative-based composites by electrospinning has been reported for enzyme immobilization [27] and multiple environmental remediation applications such as oil–water separation, oil absorption, and pollutant removal [28–31]. Cellulose acetate/silica (CA/SIL) hybrids from tetraethyl orthosilicate (TEOS)-based sol–gel processes have also been applied in preparing thermally and mechanically stable nanofiber aerogels [32] and membranes for metal ion removal [33]. Additionally, carbon nanofibers/silicon carbide composites have been prepared by electrospinning CA and silicon carbide nanoparticles, followed by deacetylation and carbonization, and proposed as reinforcements for composite materials [34]. In this study, CA/SIL composites obtained by electrospinning are explored for the first time in lubricant formulations.

On the other hand, to reduce the number of additives of different chemical natures in lubricant formulations, the challenge lies in producing multifunctional ingredients that stabilize the oil medium, impart specific rheological properties, reduce friction, and provide other functional properties, such as wear protection. Traditionally, thickening agents and multiple additives are physically blended into the base oil to achieve optimum viscosity, desired friction reduction, wear minimization, and other specific properties. Metal oxides, sulfides, and clays are often included to enhance lubricant performance, sometimes in the form of nanoparticles [35–38]. However, this traditional approach may not achieve cost-effectiveness and lubricity efficiency simultaneously. Interactions among different components can produce antagonistic effects, reducing the efficacy of additives and thickening agents and often necessitating additional additives, such as organic surfactants or dispersants, to prevent agglomeration and undesired interactions [39, 40].

The novelty of this study lies in the development of new multifunctional and environmentally friendly ingredients based on biopolymer/silica composites obtained by electrospinning, aiming to achieve more environmentally friendly semi-solid lubricant formulations and to reduce the number of components. We hypothesize that these nanocomposites will combine the benefits of both the biopolymer, CA in this case, to impart specific rheological properties, and the inorganic component, silica, to provide antifriction and/or antiwear properties in tribological contacts. The oil structuring ability of electrospun composites has been investigated through oscillatory shear rheological measurements in the linear viscoelastic regime, which are highly sensitive to changes in gel strength [41]. Additionally, the imparted anti-friction and anti-wear properties have been assessed through tribological testing. Both functionalities have been analyzed concerning the morphology of the electrospun nanostructures, the CA/SIL ratio, and the composite concentration in the resulting oleo-dispersions.

2 | Materials and Methods

2.1 | Materials

This study utilized commercial CA from Merck Sigma-Aldrich, with a number-average molecular weight of 30,000 g/mol and a degree of substitution for acetyl groups of 2.41, determined by GPC and NMR spectroscopy, respectively [40]. AEROSIL R-106 (SIL), a hydrophobic fumed silica surface treated with octamethylcyclotetrasiloxane, was supplied by Evonik, and used in addition to CA to form the electrospun composites. Dimethylacetamide (DMAc, purity ≥ 99%) from Merck Sigma-Aldrich and acetone (Ac, purity ≥ 99.5%) from Honeywell were employed as solvents. Castor oil was purchased from Guinama. Castor oil was selected on the basis of its great potential as renewable and ecofriendly basestock for lubricants [42], especially suitable as base oil in semisolid lubricants [43] due to its high viscosity and the polarity imparted by the hydroxyl groups present in the fatty chains. Moreover, castor oil is nonedible, highly available, cost-effective, and biodegradable.

2.2 | Preparation and Characterization of CA/SIL Solutions

CA and SIL powders were dissolved in a 2:1 (wt./wt.) Ac:DMAc binary solvent in different CA:SIL weight ratios (1:0, 10:1, 5:1, and 2:1) and total concentrations ranging from 0.1 to 30 wt.%. CA/SIL was dissolved after 4 h of stirring at room temperature, followed by sonication in an ultrasonic bath for 10 min. The electrical conductivity, surface tension, and dynamic viscosity of these solutions were measured at room temperature (~23 °C ± 1°C). The electrical conductivity was determined using a GLP 31 model Crison conductivity meter. The equilibrium surface tension of CA/SIL solutions was measured using a surface tensiometer (Sigma 703D, Biolin Scientific) fitted with a platinum Wilhelmy plate. The shear viscosity was determined using an ARES controlled-strain rheometer (Rheometric Scientific) with a coaxial cylinder geometry (32 mm inner diameter, 1 mm gap) in a 5–200 s^{-1} shear rate range. These physicochemical properties were replicated at least three times.

2.3 | Electrospinning Setup and Characterization of Electrospun CA/SIL Nanostructures

The CA/SIL solutions were electrospun in a chamber from DOXA Microfluidics fitted with a metallic needle syringe (inner diameter 0.80 mm) arranged horizontally in a syringe pump. The applied electrospinning processing parameters were 11–14 kV applied voltage, 0.5–0.6 mL/h feeding rate, and 15 cm tip-to-collector distance. Electrospinning was conducted at room temperature (~23 °C ± 1°C) and 45%–55% relative humidity. Electrospun nanostructures were deposited on a plate collector covered with aluminum foil. The morphologies of CA/SIL nanostructures were examined by electron microscopy (SEM) using a JXA-8200 SuperProbe (JEOL) microscope. Samples were coated with gold prior to SEM imaging. Compositional analysis of the electrospun structures was conducted through energy-dispersive X-ray spectroscopy (EDS) in a FlexSEM 1000 II microscope (Hitachi). The FIJI ImageJ software was used to analyze the SEM images of the different electrospun nanostructures. The average fiber diameter (D_f) was calculated from the fiber size distributions, as described elsewhere [44]. Additionally, the number and size of electrosprayed particles or beads were evaluated in terms of the percentage of the area they occupied in the SEM images, referred to as S_{bead}.

2.4 | Preparation and Characterization of Dispersions of the CA/SIL Nanostructures in Castor Oil

The CA/SIL nanostructures produced by electrospinning were dispersed in castor oil (placed in an open vessel) by stirring with an anchor-type impeller at a rotational speed of 60 rpm for 15 min. The concentration of the nanostructures varied from 5 to 12.5 wt%. The samples were stored for at least 24 h before being rheologically and tribologically characterized.

The rheological characterization of CA/SIL oleo-dispersions was performed using a controlled stress rheometer (Rheoscope, Thermo Haake) with a roughened stainless-steel parallel-plate geometry (35 mm, 1 mm gap). Small-amplitude oscillatory shear (SAOS) experiments were conducted in a frequency range between 0.04 and 100 rad/s at 25°C in the linear viscoelastic regime. Stress sweep tests at 1 rad/s were performed to determine the extent of the linear viscoelastic range. Samples were kept at rest for 15 min prior to measurements to avoid any residual stress history. All rheological tests were conducted at least in duplicate.

The tribological performance of CA/SIL oleo-dispersions was evaluated using a tribological cell coupled to an MCR-501 rheometer (Anton Paar), comprising a ½″ diameter steel (1.4401 grade 100 AISI 316) ball rotating on three 45° inclined rectangular steel (1.4301 AISI 304, 80 HRB hardness) plates. The stationary friction coefficient was obtained at room temperature by applying a normal load of 20 N and setting a constant angular velocity of 10 rpm for 600 s. Five replicates were performed for each test. The wear produced on the steel plates after the five replicates was analyzed using a BX51 optical microscope (Olympus), from which the average diameters of wear scars were determined.

3 | Results and Discussion

3.1 | Influence of the Spinning Solution Concentration

Table 1 presents the physicochemical properties of CA and CA/SIL solutions in the Ac:DMAc binary solvent (i.e., surface tension, electrical conductivity, and dynamic viscosity) as a function of solution concentration. The surface tension values decrease with increasing CA concentration from 25.5 to 20.7 mN/m, and the addition of silica does not significantly affect this trend. This reduction in surface tension facilitates the electrospinning process, contributing to the proper formation and stabilization of the Taylor cone and a continuous fluid jet from the syringe tip [45, 46]. The electrical conductivity initially increases with concentration up to around 7.6 μS/cm for a 10 wt.% concentration and then remains constant or slightly decreases. This behavior suggests a change in the concentration regime around this critical concentration, yielding a reduction in the mobility of solute molecules. Again, the addition of silica does not influence electrical conductivity. Finally, all CA or CA/SIL solutions exhibited a Newtonian behavior, and the viscosity increased with concentration.

To detect any change in concentration regimes, the specific viscosity, η_{sp} ($\eta_{sp} = (\eta/\eta_s) - 1$, with η_s being the solvent viscosity), was plotted against solution concentration on log–log scales (Figure 1) for CA/SIL solutions with different CA:SIL ratios. Thus, η_{sp} varies with concentration in the same way regardless of the CA:SIL ratio. A transition from the semidilute unentangled regime to the semidilute entangled regime was detected by a change in the slope at approximately the same concentration (~5.8 wt.%), known as the entanglement concentration (C_e). The scaling exponents deduced from the η_{sp} versus concentration plots corroborated these concentration regimes. Below C_e, $\eta_{sp} \sim C^{1.5}$ agrees with the scaling exponent predicted by the Rouse model for neutral polymers in good solvents in the semidilute unentangled regime. Meanwhile, $\eta_{sp} \sim C^{4.5}$ for the entangled

TABLE 1 | Surface tension, electrical conductivity, and dynamic viscosity for CA and CA/SIL solutions at different concentrations.

	Concentration (wt.%)	Surface tension (mN/m)	Electrical conductivity (μS/cm)	Dynamic viscosity (Pa s)
CA	0	25.53	1.04	6.17×10^{-4}
	0.1	—	—	6.48×10^{-4}
	1	25.64	2.61	1.46×10^{-3}
	3	24.82	3.86	4.64×10^{-3}
	5	23.91	5.98	0.014
	7	24.02	6.85	0.031
	10	25.32	7.63	0.091
	15	21.86	7.68	0.506
	20	20.76	6.94	3.299
	25	—	6.19	10.989
CA/SIL (10:1 weight ratio)	0	25.53	1.04	6.17×10^{-4}
	0.1	—	—	6.85×10^{-4}
	1	24.58	3.65	1.16×10^{-3}
	3	—	—	3.79×10^{-3}
	5	24.09	5.94	0.011
	7	—	—	0.023
	10	23.01	7.63	0.076
	13	—	—	0.226
	15	21.00	7.59	0.386
	17	—	—	0.675
	20	20.48	7.23	1.694
	23	—	—	3.930
	25	18.24	7.05	6.551

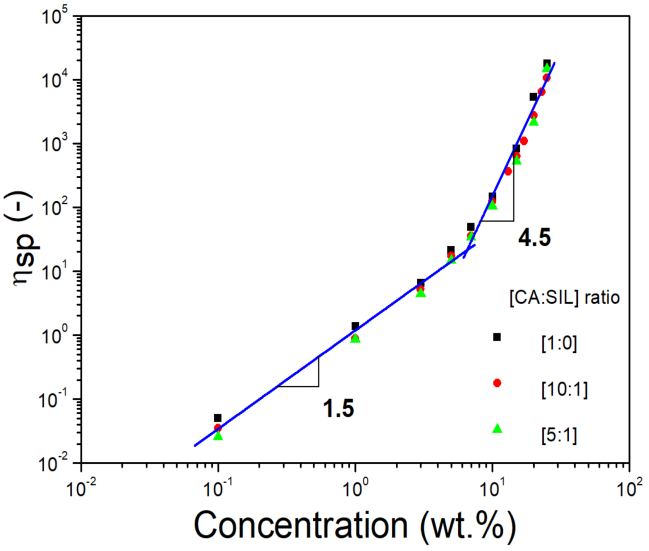

FIGURE 1 | Influence of spinning solution concentration on the specific viscosity of CA and CA/SIL solutions for three different CA:SIL ratios.

regime is also consistent with the predicted ~x3 scaling exponent value above C_e [47].

The C_e has been correlated with the electrospinnability of polymer solutions and the resulting morphologies of electrospun structures [21, 48, 49]. It has been reported that to obtain homogeneous nanofiber mats, the spinning solution concentration should be at least 2–2.5 times C_e. Different fiber morphologies, such as particles interconnected with thin filaments, beaded fibers, and uniform bead-free fibers, have been associated with different polymer concentration regimes [18, 21, 48], which agrees with the results obtained in this study. As shown in Figure 2a,b, the morphology of electrospun CA/SIL nanostructures evolves from micro-sized particles connected by thin filaments at a 10 wt.% concentration to beaded fibers and then uniform bead-free nanofiber mats as the solution concentration increases to around 17–20 wt.%, i.e., above 2.5 times C_e.

However, as discussed below, the transition from beaded fibers to relatively homogeneous fiber mats is slightly delayed

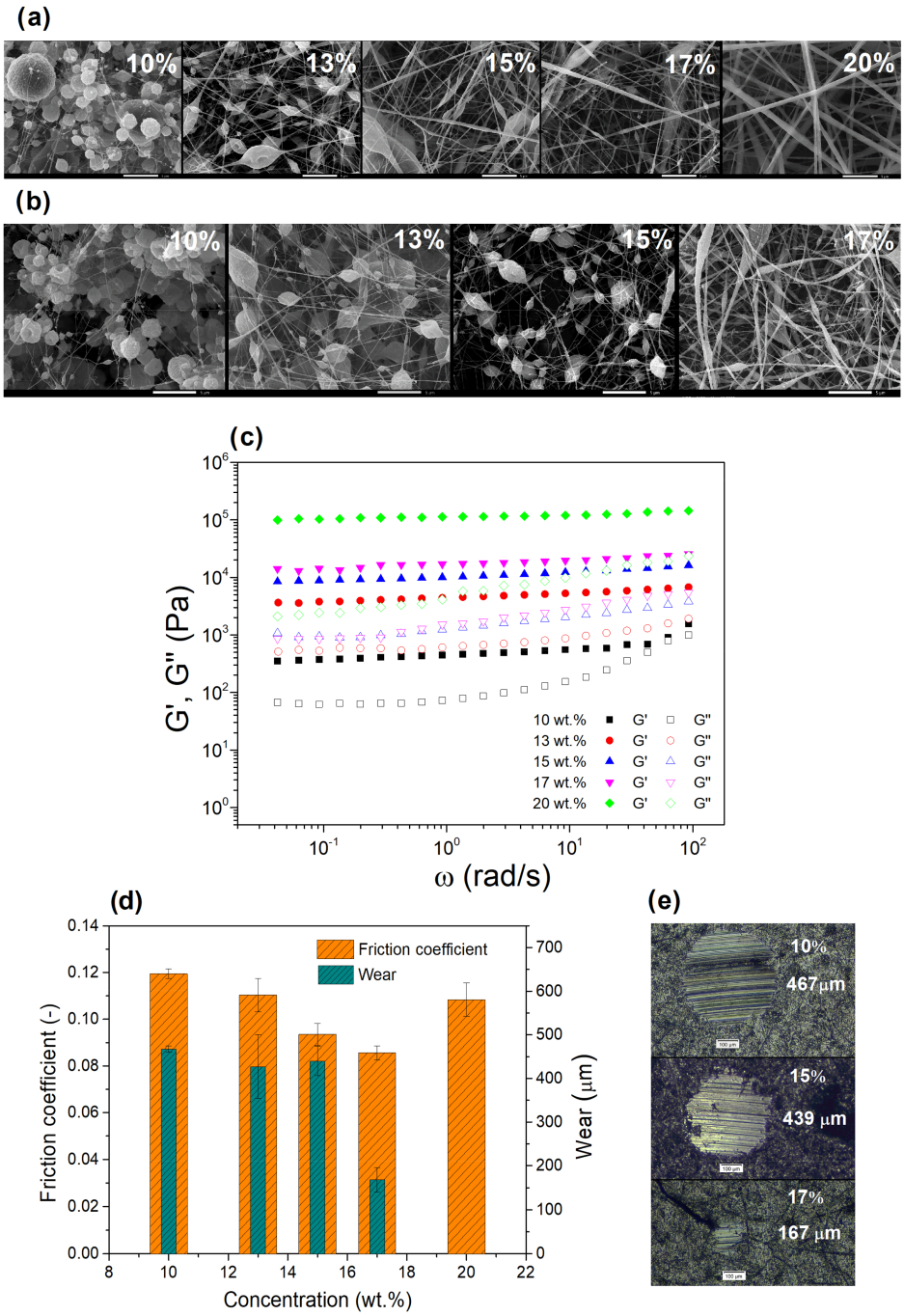

FIGURE 2 | Influence of spinning solution concentration on (a,b) the morphology of electrospun CA/SIL nanostructures for 10:1 (a) and 5:1 (b) CA:SIL weight ratios (5000× magnification); (c) the linear viscoelastic response of oleo-dispersions of CA/SIL composites in castor oil (10 wt.% nanofibers in castor oil, 10:1 CA:SIL weight ratio); (d) the friction coefficient values and average wear scar diameters produced in the steel plates of the tribological contact (10 wt.% nanofibers in castor oil, 10:1 CA:SIL weight ratio); and (e) selected images of these wear scars.

(i.e., achieved at higher concentrations) as the CA:SIL ratio decreases. In all cases, SIL is uniformly distributed throughout the nanostructure. Furthermore, the compositional analysis agrees with the CA:SIL proportion introduced in the spinning solution, as shown in Figure 3, where the results of the EDS analysis are included for a selected composite.

Once the electrospun CA/SIL nanostructures were dispersed in castor oil, the morphology of the nanostructures was apparently preserved with a certain degree of swelling (around 25%) (see Figure S1), as previously reported for dispersions of electrospun kraft lignin/CA nanofibers in castor oil [20]. A similar effect was observed in electrospun CA nanofibers incorporating high loads (i.e., 20 wt.%) of an essential oil [50]. Figure 2c shows the rheological response of the resulting gel-like systems obtained by dispersing the CA/SIL electrospun nanostructures in castor oil at 10 wt.%. The mechanical spectra of these oleo-dispersions are qualitatively similar regardless of the CA/SIL concentration in the electrospinning solution. In all cases, there was a predominant

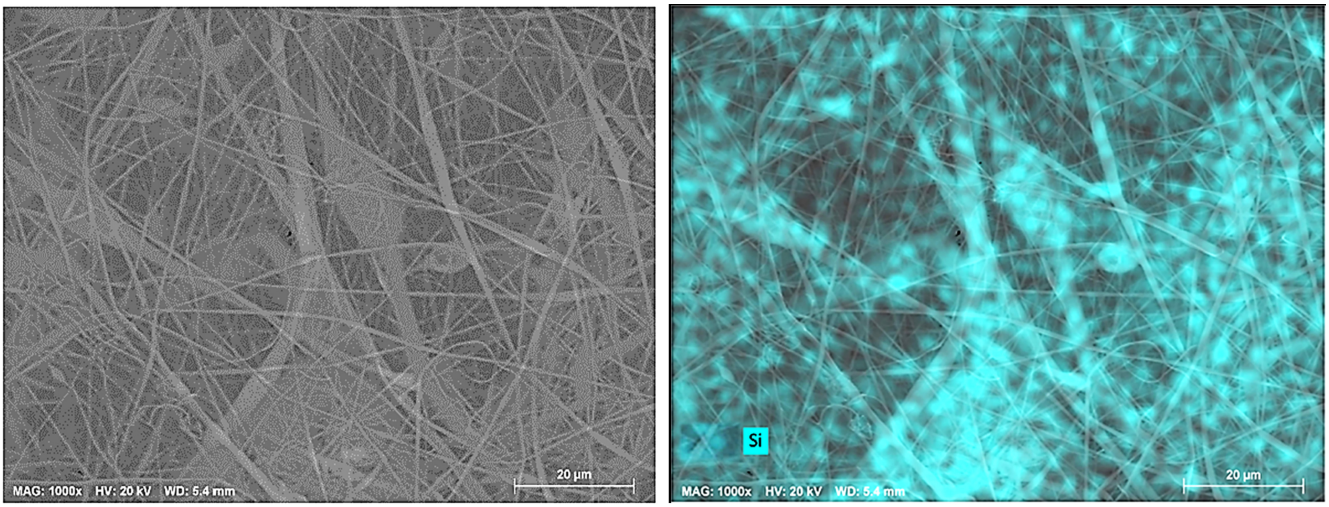

	Theoretical (wt. %)	Experimental (wt. %)
C	47.44	49.68 ± 6.49
O	48.24	44.83 ± 6.07
Si	4.32	5.49 ± 0.27

FIGURE 3 | EDS compositional analysis for a selected electrospun CA/SIL composite (17 wt.% spinning solution concentration and 10:1 CA:SIL ratio). The light blue color in the SEM image represents the distribution of Si. The theoretical elemental composition refers to the CA:SIL proportion introduced in the spinning solution, while the experimental data are those obtained from the EDS analysis.

elastic response where the storage modulus (G′) is higher than the loss modulus (G″) in the entire frequency range studied, with G′ being almost independent of frequency and G″ displaying a minimum, known as the "plateau" region of the mechanical spectrum. The "plateau" region is typically found in colloidal gel-like dispersions, such as conventional lubricating greases [51], and entangled polymeric systems [52]. In this case, the "plateau" region reflects the packing effect in the percolation network formed by electrospun fibers. The plateau modulus (G_N^0) defined elsewhere [52] is the characteristic parameter of this plateau region, which may be interpreted as a measure of gel strength.

Despite the very similar evolution of both SAOS functions with frequency, the morphology of the electrospun nanostructure greatly influences the magnitude of both G′ and G″. Both moduli increased by almost two orders of magnitude when the concentration of the spinning solution was raised from 10 to 20 wt.%. Therefore, although micro-particles interconnected by thin filaments can stabilize the oleo-dispersion, providing a gel-like rheological behavior, more homogeneous structures predominantly comprising larger nanofibers produced dispersions with much higher gel strength. Comparable oil structuring ability has been previously reported when using electrospun nanofibers of CA phthalate [53] or lignin-rich lignocellulosic residues [54] as structurants, where very similar ranges of values for the SAOS functions were provided when transitioning from fiber-bead structures to well-developed nanofibers.

In fact, G_N^0 values can be correlated with a product of powers of the average fiber diameter (D_f) and the fraction of the area occupied by particles or beads (S_{bead}), as shown in Figure 4a, with D_{f} having a much higher weight than S_{bead} (i.e., power-law exponents of 3 and −0.25, respectively). The values of these power-law exponents were obtained from an optimal linearization of the evolution of G_N^0 with this power series, representing the best linear regression.

Furthermore, the lubrication performance of these gel-like oleo-dispersions was evaluated in a steel–steel ball-on-plates tribological contact under pure sliding conditions by applying a constant rotational speed and normal load (10 rpm and 20 N, respectively) and monitoring the friction coefficient over time. Figure 2d shows the values of the stationary friction coefficient obtained and the average diameter of the wear scars produced on the steel plates. Meanwhile, Figure 2e shows selected images of these wear marks. The friction coefficient was significantly reduced by increasing the spinning solution concentration from 10 to 17 wt.%. This indicates that CA/SIL nanofiber composites are more effective in reducing friction than microparticles or beaded fibers. This likely occurs because nanofibers may penetrate into the contact more easily than particles, increasing the film thickness and thereby preventing wear to a greater extent. Conversely, we hypothesize that particles and beaded fibers have more difficulty entering the tribological contact, likely accumulating at the inlet points. However, the dispersion of homogeneous but thicker nanofibers was achieved with a 20 wt.% solution and produced slightly higher friction than other more irregular nanostructures obtained with solutions at 15 or 17 wt.%, although it provided full wear protection (i.e., no wear scars were detected on the steel plates).

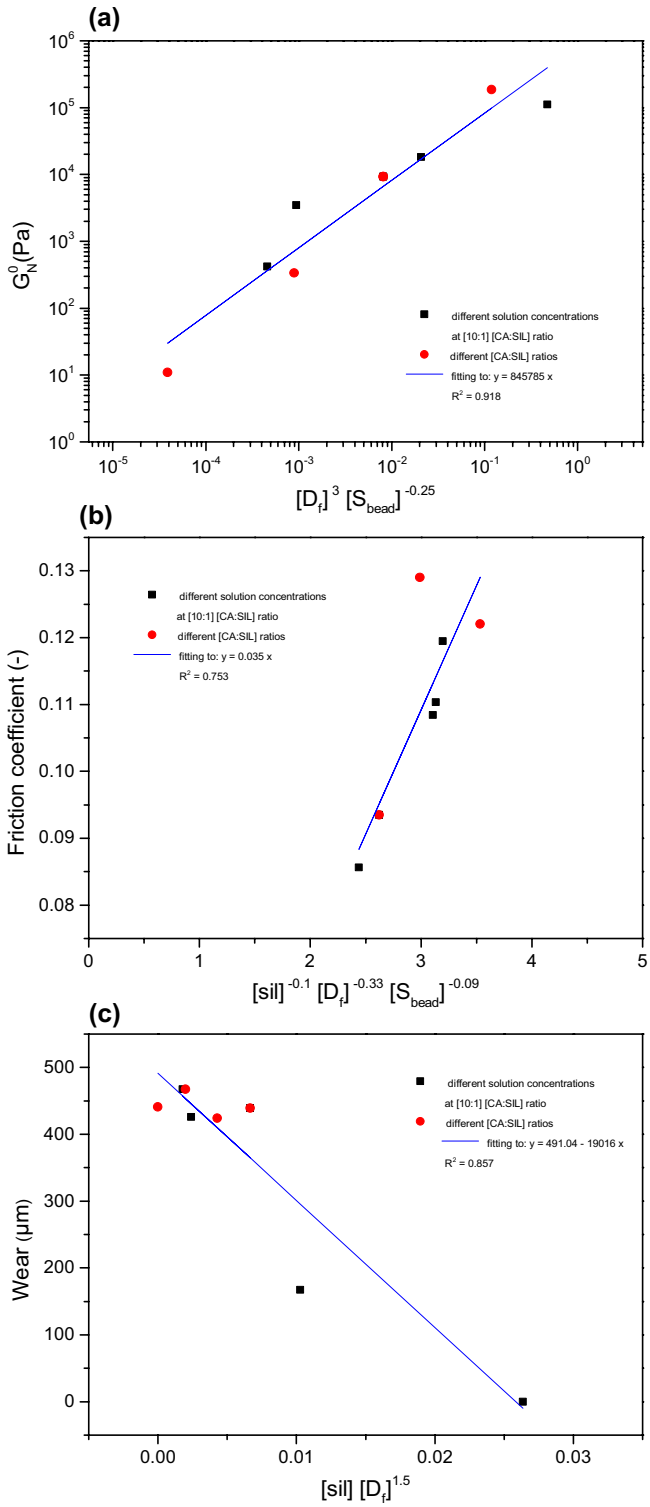

FIGURE 4 | Correlations between (a) the plateau modulus, (b) the friction coefficient, and (c) the wear scar size, and power series of the average fiber diameter (D_f), the fraction of area occupied by particles or beads (S_{bead}), and the SIL weight fraction introduced in the composites (*sil*).

3.2 | Influence of CA:SIL Ratio

Combining a biopolymer like CA and an inorganic oxide like SIL in a single nanocomposite may provide desirable multifunctional properties, acting as an oil structuring agent and offering antifriction and/or antiwear properties. Figure 5a shows the influence of the CA:SIL ratio on the electrospinnability of CA/SIL solutions at a 15 wt.% concentration. As expected, the uniform nanofiber mats obtained with the CA solution became progressively distorted as the silica proportion increased, resulting in beaded fibers or even electrosprayed particles interconnected with thin filaments for a 2:1 CA:SIL weight ratio. This significantly impacts the oil structuring properties of these composites. As shown in Figure 5b, the values of the SAOS functions vary by approximately four orders of magnitude when SIL is introduced into the nanofibers and the CA:SIL weight ratio decreases to 2:1. This result is consistent with the reduced tensile strength reported for CA/SIL composites obtained by casting at high silica contents [24], considering that a direct correlation between the mechanical properties of electrospun nanofibers and the rheological properties of the resulting oleogels has been demonstrated in the case of lignocellulose/PET composites [55].

Moreover, the extended plateau region found for the oleo-dispersions of composites with high CA:SIL ratios is shortened when using particle-dominated structures, yielding a crossover between G′ and G″ at intermediate frequencies for a 2:1 CA:SIL weight ratio. This effect was also previously found when using electrospun cellulose acetate-phthalate nanostructures of different morphology as thickeners [53] The mechanical spectrum of the oleo-dispersion of pure CA nanofibers (see Figure 5b) is comparable to that obtained with the electrospun CA/SIL composite (10:1 weight ratio) from a 20 wt.% solution concentration (see Figure 2c). This supports the idea that the oil structuring ability of these composites is mainly due to the morphological properties achieved by electrospinning, regardless of the CA:SIL ratio. Indeed, G_N^0 values of the dispersions of electrospun composites with different CA:SIL ratios correlate perfectly with the power function of D_f and S_{bead} previously discussed (see Figure 4a).

However, for similar nanoarchitectures and rheological responses, introducing silica in the nanocomposite significantly reduces both friction and wear (see, for instance, the values of friction coefficient and average wear scar diameters in Figures 2d and 5c for the oleo-dispersions formulated with CA/SIL and CA nanofibers obtained from 20 to 15 wt.% solution concentrations, respectively). Thus, introducing silica in a 10:1 CA:SIL ratio reduced friction by approximately 52% compared with the SIL-free CA oleo-dispersion, while wear was completely prevented.

Nonetheless, the effect of the CA:SIL ratio on the lubrication performance of the resulting oleo-dispersions is more complex. On one hand, as discussed above, adding SIL significantly reduces both friction and wear compared with the SIL-free CA nanofibers. On the other hand, a further increase in SIL content hinders the production of nanofibers, as shown in Figure 5a, which may result in detrimental effects on both the friction coefficient and wear scar size. For instance, for oleo-dispersions of 10 wt.% composites obtained from solutions at 15 wt.%, Figure 5c shows that the friction coefficient was significantly reduced (roughly 59%), by introducing a small proportion of silica (10:1 CA:SIL ratio) compared with the SIL-free CA nanofibers. Such a reduction

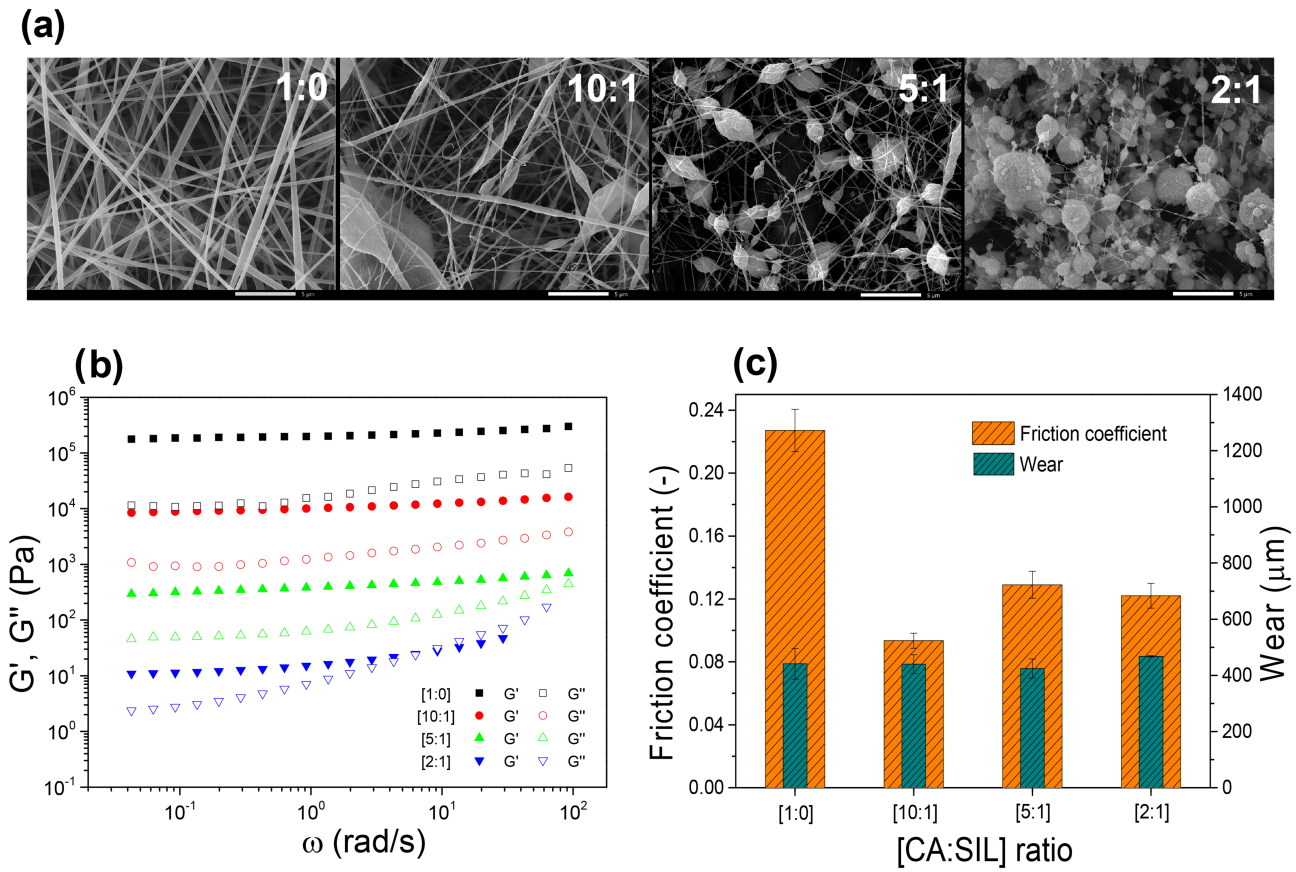

FIGURE 5 | Influence of the CA:SIL weight ratio on (a) the morphology of electrospun CA/SIL nanostructures (15 wt.% spinning solution concentration, 5000× magnification); (b) the linear viscoelastic response of the resulting oleo-dispersions of CA/SIL composites in castor oil (10 wt.% nanofibers); and (c) the friction coefficient values and average wear scar diameters produced in the steel plates of the tribological contact (10 wt.% nanofibers in castor oil).

in the friction coefficient is much greater than that achieved by introducing, in a similar proportion, graphene nanoparticles in lithium greases [56] or $ZnFe_2O_4$@C/graphene oxide nanocomposites in a polyalphaolefin oil [57] and similar to that reported for black phosphorus/Fe_3O_4 nanocomposites used as antifriction additive in soybean oil [58] However, the friction coefficient slightly increased with a further reduction in the CA:SIL ratio, while no significant differences were found in wear scar dimensions. This must again be explained based on the different morphologies achieved.

To discriminate the effects of both the morphological properties of electrospun composites and the SIL fraction introduced, namely "sil," the friction coefficient was also correlated with a product of powers of D_f, S_{bead}, and *sil* (see Figure 4b), corroborating that the *sil* parameter contributes positively to friction reduction, that is, a negative power-law exponent. On the other hand, the influence of fiber diameter (D_f) on the friction coefficient is roughly three times larger than those deduced for S_{bead} and *sil* (see exponents of the power series on the *x*-axis). However, it is worth noting that only SIL-containing nanostructures were considered in Figure 4b and, therefore, the drastic reduction in the friction coefficient observed when introducing a small proportion of SIL in CA nanofibers, as previously discussed, is not illustrated in this graph. Finally, according to this correlation, the presence of beads in the nanofibers also has an unexpected positive influence in reducing friction, which may be related to the capacity of these beaded fibers to increase the film thickness if they can eventually penetrate into the lubricated contact, similar to the effect of increasing D_f. In contrast, wear reduction exclusively depends on the SIL content and nanofiber diameter, as shown in Figure 4c. In summary, the improvement in lubrication performance results from a balance between incorporating SIL into the nanocomposites and achieving well-developed and thick nanofibers by electrospinning, the latter being hindered by decreasing the CA:SIL ratio.

3.3 | Influence of CA/SIL Composite Concentration in the Oleo-Dispersions

In the lubricant industry, grease consistency is typically controlled by adjusting the thickener concentration [59]. Figure 6a shows the mechanical spectra of oleo-dispersions of a selected CA/SIL composite predominantly comprising nanofibers (10:1 CA:SIL weight ratio, 17% spinning solution concentration) at different concentrations. Despite the very similar evolution of the SAOS functions with frequency (i.e., the plateau region of the mechanical spectrum), the consistency of the gel-like dispersion increased with nanofiber concentration as expected. This is reflected in a significant increase in the values of the SAOS functions by almost two decades as the composite

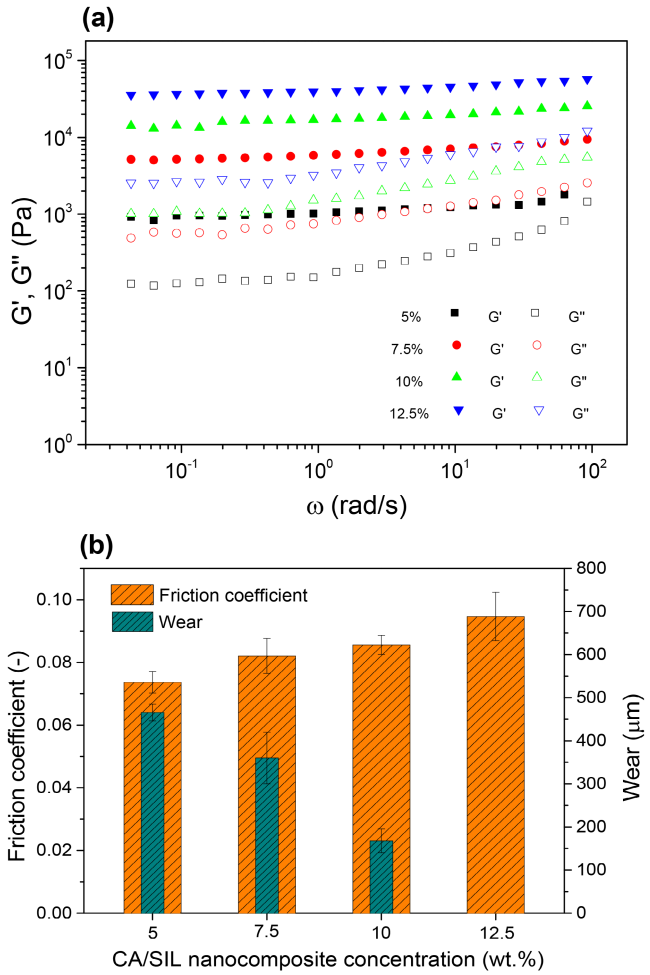

FIGURE 6 | Influence of the CA/SIL composite concentration on (a) the linear viscoelastic response of oleo-dispersions and (b) the friction coefficient values and average wear scar diameters produced in steel-steel ball-on-three plates tribological contact. The selected composite corresponds to a 17 wt.% spinning solution concentration and a 10:1 CA:SIL weight ratio.

concentration increased from 5 to 12.5 wt.%. It is worth noting that conventional metal soap-thickened NLGI 1–2 greases generally require higher thickener concentrations (above 12–14 wt.%) to achieve G′ values in the range of 10^4–10^5 Pa [60, 61].

Regarding the tribological response (see Figure 6b), the friction coefficient slightly increases with composite concentration, an expected result since, in the mixed lubrication regime, the internal friction contribution of greases increases with thickener concentration [62–64]. However, wear was significantly reduced by increasing the composite concentration, probably due to an increase in the lubricant film thickness, yielding full wear protection at a 12.5 wt.% concentration, where no wear scars were detected on the steel plates. It is worth mentioning that these oleo-dispersions used as lubricants provided significantly lower friction coefficient values and comparable or even better wear protection than fully formulated commercial greases thickened with lithium and calcium soaps tested under similar conditions [17, 51]. For instance, the oleo-dispersion containing 10 wt.% of the composite with a 10:1 CA:SIL weight ratio offers better tribological performance (i.e., antifriction and antiwear properties) than these commercial lubricating greases, which presumably contain higher thickener contents and packages of multiple additives.

4 | Conclusions

This study demonstrates the effectiveness of electrospun CA/SIL composites as multifunctional ingredients in castor oil-based semisolid lubricant formulations. CA/SIL nanocomposites confer several functionalities, including appropriate oil structuring ability and excellent anti-friction and anti-wear properties for the ultimate lubricant formulation. The adequate multifunctional activity of CA/SIL nanocomposites results from a critical balance between incorporating silica into the composites and achieving nanofiber-dominated structures through electrospinning. This balance is challenged by the increasing proportion of silica in the composites.

The oil structuring ability of these nanocomposites is primarily due to the morphological properties achieved by electrospinning, irrespective of the CA:SIL ratio. The linear viscoelastic functions of the oleo-dispersions increase with the average fiber diameter and decrease with the number and size of embedded microparticles or beads. Conversely, the introduction of silica into the nanofibers significantly improved the anti-friction and anti-wear properties. The lubrication performance is enhanced by increasing the silica content and producing nanofiber-dominated structures through electrospinning. Both effects must be balanced by adjusting the concentration of the spinning solution and the CA:SIL ratio. For similar nanoarchitectures and rheological responses, friction is reduced by approximately 52% by introducing silica in a 10:1 CA:SIL ratio. Meanwhile, wear was completely prevented compared with the oleo-dispersion of SIL-free electrospun CA nanofibers.

Increasing the composite concentration enhances gel strength and wear protection despite a slight expected increase in the friction coefficient. A 12.5 wt.% concentration of a composite predominantly comprising nanofibers with a 10:1 CA:SIL ratio yields full wear protection.

Overall, dispersing electrospun CA/SIL composites in castor oil at relatively low concentrations achieves rheological behavior and lubrication performance comparable to those found in fully formulated commercial greases.

Author Contributions

Manuel Toro-Gallego: data curation (lead), formal analysis (equal), investigation (equal), methodology (equal), validation (equal), writing – review and editing (supporting). **Concepción Valencia:** conceptualization (equal), formal analysis (equal), investigation (equal), methodology (equal), supervision (equal), validation (equal), writing – review and editing (supporting). **M. Carmen Sánchez:** conceptualization (equal), investigation (equal), methodology (equal), validation (equal), writing – review and editing (supporting). **José E. Martín-Alfonso:** conceptualization (equal), funding acquisition (equal), investigation (equal), methodology (equal), supervision (equal), writing – review and editing

(supporting). **José M. Franco:** conceptualization (equal), funding acquisition (lead), investigation (equal), methodology (equal), project administration (lead), supervision (lead), writing – original draft (lead), writing – review and editing (lead).

Acknowledgments

This work is part of the Research Project PID2021-125637OB-I00, funded by MICIU/AEI/10.13039/501100011033 and by ERDF/EU. Funding is gratefully acknowledged. Open Access funding provided by Universidad de Huelva/CBUA thanks to the CRUE-CSIC agreement with Wiley.

Conflicts of Interest

The authors declare no conflicts of interest.

Data Availability Statement

The corresponding author will make all the data and materials available upon reasonable request.

References

1. J. Luo and X. Zhou, "Superlubricitive Engineering—Future Industry Nearly Getting Rid of Wear and Frictional Energy Consumption," *Friction* 8 (2020): 643–665.

2. Y. Meng, J. Xu, Z. Jin, B. Prakash, and Y. Hu, "A Review of Recent Advances in Tribology," *Friction* 8 (2020): 221–300.

3. B. Kohlhauser, M. R. Ripoll, H. Riedl, et al., "How to Get noWear? – A New Take on the Design of In-Situ Formed High Performing Low-Friction Tribofilms," *Materials and Design* 190 (2020): 108519.

4. G. Moreno, J. M. Franco, C. Valencia, and C. Gallegos, "Rheology of Lubricating Greases Modified With Reactive NCO-Terminated Polymeric Additives," *Journal of Applied Polymer Science* 118 (2010): 693–704.

5. B. G. P. van Ravensteijn, R. Bou Zerdan, D. Seo, et al., "Triple Function Lubricant Additives Based on Organic–Inorganic Hybrid Star Polymers: Friction Reduction, Wear Protection, and Viscosity Modification," *ACS Applied Materials & Interfaces* 11 (2019): 1363–1375.

6. S. Wen and P. Huang, "Boundary Lubrication and Additives," in *Principles of Tribology* (Beijing: Tsinghua University Press, Wiley, 2017), 171.

7. R. K. Singh, A. Kukrety, and A. K. Singh, "Study of Novel Ecofriendly Multifunctional Lube Additives Based on Pentaerythritol Phenolic Ester," *ACS Sustainable Chemistry & Engineering* 2014 (1959): 2–1967.

8. T. M. Panchal, A. Patel, D. D. Chauhan, M. Thomas, and J. V. Patel, "A Methodological Review on Bio-Lubricants From Vegetable Oil Based Resources," *Renewable and Sustainable Energy Reviews* 70 (2017): 65–70.

9. A. Z. Syahir, N. W. M. Zulkifli, H. H. Masjuki, et al., "A Review on Bio-Based Lubricants and Their Applications," *Journal of Cleaner Production* 168 (2017): 997–1016.

10. A. M. Danilov, S. A. Antonov, R. V. Bartko, and P. A. Nikulshin, "Recent Advances in Biodegradable Lubricating Materials (A Review)," *Petroleum Chemistry* 61 (2021): 697–710.

11. T. Xia, Y. Huang, P. Lan, L. Lan, and N. Lin, "Physical Modification of Cellulose Nanocrystals With a Synthesized Triblock Copolymer and Rheological Thickening in Silicone Oil/Grease," *Biomacromolecules* 20 (2019): 4457–4465.

12. Z. Wu, P. P. Thoresen, L. Matsakas, U. Rova, P. Christakopoulos, and Y. Shi, "Facile Synthesis of Lignin-Castor Oil-Based Oleogels as Green Lubricating Greases With Excellent Lubricating and Antioxidation Properties," *ACS Sustainable Chemistry & Engineering* 11 (2023): 12552–12561.

13. R. Sánchez, G. B. Stringari, J. M. Franco, C. Valencia, and C. Gallegos, "Use of Chitin, Chitosan and Acylated Derivatives as Thickener Agents of Vegetable Oils for Bio-Lubricant Applications," *Carbohydrate Polymers* 85 (2011): 705–714.

14. E. Cortés-Triviño, C. Valencia, M. A. Delgado, and J. M. Franco, "Rheology of Epoxidized Cellulose Pulp Gel-Like Dispersions in Castor Oil: Influence of Epoxidation Degree and the Epoxide Chemical Structure," *Carbohydrate Polymers* 199 (2018): 563–571.

15. J. E. Martín-Alfonso, N. Núñez, C. Valencia, J. M. Franco, and M. J. Díaz, "Formulation of New Biodegradable Lubricating Greases Using Ethylated Cellulose Pulp as Thickener Agent," *Journal of Industrial and Engineering Chemistry* 17 (2011): 818–823.

16. R. Gallego, J. F. Arteaga, C. Valencia, M. J. Díaz, and J. M. Franco, "Gel-Like Dispersions of HMDI-Cross-Linked Lignocellulosic Materials in Castor Oil: Toward Completely Renewable Lubricating Grease Formulations," *ACS Sustainable Chemistry & Engineering* 3 (2015): 2130–2141.

17. R. Gallego, T. Cidade, R. Sánchez, C. Valencia, and J. M. Franco, "Tribological Behaviour of Novel Chemically Modified Biopolymer-Thickened Lubricating Greases Investigated in a Steel–Steel Rotating Ball-On-Three Plates Tribology Cell," *Tribology International* 94 (2016): 652–660.

18. M. Borrego, J. E. Martín-Alfonso, C. Valencia, M. D. C. Sánchez Carrillo, and J. M. Franco, "Developing Electrospun Ethylcellulose Nanofibrous Webs: An Alternative Approach for Structuring Castor Oil," *ACS Applied Polymer Materials* 4 (2022): 7217–7227.

19. J. F. Rubio-Valle, M. C. Sánchez, C. Valencia, J. E. Martín-Alfonso, and J. M. Franco, "Production of Lignin/Cellulose Acetate Fiber-Bead Structures by Electrospinning and Exploration of Their Potential as Green Structuring Agents for Vegetable Lubricating Oils," *Industrial Crops and Products* 188 (2022): 115579.

20. J. F. Rubio-Valle, C. Valencia, M. Sánchez, J. E. Martín-Alfonso, and J. M. Franco, "Oil Structuring Properties of Electrospun Kraft Lignin/Cellulose Acetate Nanofibers for Lubricating Applications: Influence of Lignin Source and Lignin/Cellulose Acetate Ratio," *Cellulose* 30 (2023): 1553–1566.

21. M. A. Martín-Alfonso, J. F. Rubio-Valle, J. E. Martín-Alfonso, and J. M. Franco, "Oleo-Dispersions of Electrospun Cellulose Acetate Butyrate Nanostructures: Toward Renewable Semisolid Lubricants," *Advanced Sustainable Systems* 8 (2024): 2300592.

22. W. Zhang, Z. He, Y. Han, et al., "Structural Design and Environmental Applications of Electrospun Nanofibers," *Composites. Part A, Applied Science and Manufacturing* 137 (2020): 106009.

23. A. M. Dobos, A. Filimon, A. Bargan, and M. F. Zaltariov, "New Approaches for the Development of Cellulose Acetate/Tetraethyl Orthosilicate Composite Membranes: Rheological and Microstructural Analysis," *Journal of Molecular Liquids* 309 (2020): 113129.

24. A. M. Dobos, A. Bargan, S. Dunca, C. M. Rîmbu, and A. Filimon, "Cellulose Acetate/Silica Composites: Physicochemical and Biological Characterization," *Journal of the Mechanical Behavior of Biomedical Materials* 144 (2023): 106002.

25. J. P. Reddy, A. Varada Rajulu, J. W. Rhim, and J. Seo, "Mechanical, Thermal, and Water Vapor Barrier Properties of Regenerated Cellulose/Nano-SiO2 Composite Films," *Cellulose* 25 (2018): 7153–7165.

26. Y. Sun, J. Bai, Z. Wang, H. Li, and H. Dong, "A Hydrophobic/Oleophilic Silica-Cellulose Composite Aerogel for Oil–Water Separation," *Journal of Applied Polymer Science* 140 (2023): e54408.

27. J. Zhang, M. Song, X. Wang, et al., "Preparation of a Cellulose Acetate/Organic Montmorillonite Composite Porous Ultrafine Fiber Membrane for Enzyme Immobilization," *Journal of Applied Polymer Science* 133 (2016): 43818.

28. S. Koushkbaghi, S. Jamshidifard, A. ZabihiSahebi, A. Abouchenari, M. Darabi, and M. Irani, "Synthesis of Ethyl Cellulose/Aluminosilicate Zeolite Nanofibrous Membranes for Oil–Water Separation and Oil Absorption," *Cellulose* 26 (2019): 9787–9801.

29. P. Tsekova and O. Stoilova, "Fabrication of Electrospun Cellulose Acetate/Nanoclay Composites for Pollutant Removal," *Polymers (Basel)* 14 (2022): 5070.

30. S. Kumarage, I. Munaweera, C. Sandaruwan, L. Weerasinghe, and N. Kottegoda, "Electrospun Amine-Functionalized Silica Nanoparticles–Cellulose Acetate Nanofiber Membranes for Effective Removal of Hardness and Heavy Metals (As(v), cd(Ii),pb(Ii)) in Drinking Water Sources," *Environmental Science: Water Research & Technology* 9 (2023): 2664–2679.

31. J. Cai, M. Lei, Q. Zhang, et al., "Electrospun Composite Nanofiber Mats of Cellulose@Organically Modified Montmorillonite for Heavy Metal Ion Removal: Design, Characterization, Evaluation of Absorption Performance," *Composites. Part A, Applied Science and Manufacturing* 92 (2017): 10–16.

32. T. Pirzada, Z. Ashrafi, W. Xie, and S. A. Khan, "Cellulose Silica Hybrid Nanofiber Aerogels: From sol–Gel Electrospun Nanofibers to Multifunctional Aerogels," *Advanced Functional Materials* 30 (2020): 1907359.

33. A. A. Taha, Y. N. Wu, H. Wang, and F. Li, "Preparation and Application of Functionalized Cellulose Acetate/Silica Composite Nanofibrous Membrane via Electrospinning for Cr(VI) ion Removal From Aqueous Solution," *Journal of Environmental Management* 112 (2012): 10–16.

34. Q. Li, Y. Zhu, and S. J. Eichhorn, "Carbonized electrospun cellulose composite nanofibres containing silicon carbide nanoparticles," *Composites. Part A, Applied Science and Manufacturing* 123 (2019): 71–78.

35. A. Guerrero-Martínez, J. Pérez-Juste, and L. M. Liz-Marzán, "Recent Progress on Silica Coating of Nanoparticles and Related Nanomaterials," *Advanced Materials* 22 (2010): 1182–1195.

36. G. W. Stachowiak and A. W. Batchelor, *Engineering Tribology*, 4th ed. (Oxford: Elsevier Butterworth-Heinemann, 2013).

37. A. Hernández Battez, R. González, J. L. Viesca, et al., "CuO, ZrO_2 and ZnO Nanoparticles as Antiwear Additive in Oil Lubricants," *Wear* 265 (2008): 422–428.

38. Z. J. Zhang, D. Simionesie, and C. Schaschke, "Graphite and Hybrid Nanomaterials as Lubricant Additives," *Lubricants* 2 (2014): 44–65.

39. Y. Chen, P. Renner, and H. Liang, "Dispersion of Nanoparticles in Lubricating Oil: A Critical Review," *Lubricants* 7 (2019): 7.

40. G. Paul, H. Hirani, T. Kuila, and N. C. Murmu, "Nanolubricants Dispersed With Graphene and Its Derivatives: An Assessment and Review of the Tribological Performance," *Nanoscale* 11 (2019): 3458–3483.

41. E. Moghimi, A. R. Jacob, N. Koumakis, and G. Petekidis, "Colloidal Gels Tuned by Oscillatory Shear," *Soft Matter* 13 (2017): 2371–2383.

42. S. Asadauskas, J. H. Perez, and J. L. Duda, "Lubrication Properties of Castor Oil–Potential Basestock for Biodegradable Lubricants," *Tribology & Lubrication Technology* 53 (1997): 35.

43. M. C. Dwivedi and S. Sapre, "Total Vegetable-Oil Based Greases Prepared From Castor Oil," *Journal of Synthetic Lubrication* 19 (2002): 229–241.

44. D. Ibarra, L. García-Fuentevilla, J. F. Rubio-Valle, R. Martín-Sampedro, C. Valencia, and M. E. Eugenio, "Kraft Lignins From Different Poplar Genotypes Obtained by Selective Acid Precipitation and Their Use for the Production of Electrospun Nanostructures," *Reactive and Functional Polymers* 191 (2023): 105685.

45. D. Fang, Y. Liu, S. Jiang, J. Nie, and G. Ma, "Effect of Intermolecular Interaction on Electrospinning of Sodium Alginate," *Carbohydrate Polymers* 85 (2011): 276–279.

46. G. H. McKinley and A. Tripathi, "How to Extract the Newtonian Viscosity From Capillary Breakup Measurements in a Filament Rheometer," *Journal of Rheology* 44 (2000): 653–670.

47. R. H. Colby, "Structure and Linear Viscoelasticity of Flexible Polymer Solutions: Comparison of Polyelectrolyte and Neutral Polymer Solutions," *Rheologica Acta* 49 (2010): 425–442.

48. M. G. McKee, G. L. Wilkes, R. H. Colby, and T. E. Long, "Correlations of Solution Rheology With Electrospun Fiber Formation of Linear and Branched Polyesters," *Macromolecules* 37 (2004): 1760–1767.

49. R. R. Klossner, H. A. Queen, A. J. Coughlin, and W. E. Krause, "Correlation of Chitosan's Rheological Properties and Its Ability to Electrospin," *Biomacromolecules* 9 (2008): 2947–2953.

50. S. Beikzadeh, A. Akbarinejad, S. Swift, J. Perera, P. A. Kilmartin, and J. Travas-Sejdic, "Cellulose Acetate Electrospun Nanofibers Encapsulating Lemon Myrtle Essential Oil as Active Agent With Potent and Sustainable Antimicrobial Activity," *Reactive and Functional Polymers* 157 (2020): 104769.

51. R. Sánchez, C. Valencia, and J. M. Franco, "Rheological and Tribological Characterization of a New Acylated Chitosan–Based Biodegradable Lubricating Grease: A Comparative Study With Traditional Lithium and Calcium Greases," *Tribology Transactions* 57 (2014): 445–454.

52. M. Baurngaertel, M. E. De Rosa, J. Machado, M. Masse, and H. H. Winter, "The Relaxation Time Spectrum of Nearly Monodisperse Polybutadiene Melts," *Rheologica Acta* 31 (1992): 75–82.

53. M. A. Martín-Alfonso, J. E. Martín-Alfonso, J. F. Rubio-Valle, J. P. Hinestroza, and J. M. Franco, "Tunable Architectures of Electrospun Cellulose Acetate Phthalate Applied as Thickeners in Green Semisolid Lubricants," *Applied Materials Today* 36 (2024): 102030.

54. J. F. Rubio-Valle, C. Valencia, J. E. Martín-Alfonso, and J. M. Franco, "Valorization of Lignin-Rich Solid Residues From Different Eucalyptus Wood Conversion Processes as Oil Structurants via Electrospinning," *Industrial Crops and Products* 222 (2024): 119442.

55. J. F. Rubio-Valle, C. Valencia, M. C. Sánchez, J. E. Martín-Alfonso, and J. M. Franco, "Upcycling Spent Coffee Grounds and Waste PET Bottles Into Electrospun Composite Nanofiber Mats for Oil Structuring Applications," *Resources, Conservation and Recycling* 199 (2023): 107261.

56. Z. Li, Q. He, S. Du, and Y. Zhang, "Effect of Few Layer Graphene Additive on the Tribological Properties of Lithium Grease," *Lubrication Science* 32 (2020): 333–343.

57. B. Wu, Z. Yuan, Q. Wu, F. Qiu, C. Li, and X. Hu, "$ZnFe_2O_4$@C/Graphene Oxide Nanocomposites Designed for Enhancing the Friction Reduction Property of Lubricants," *Journal of Industrial and Engineering Chemistry* 133 (2024): 588–598.

58. H. Yu, M. Li, J. Sun, J. Su, and F. Su, "Friction-Reducing and Anti-Wear Mechanism of BP/Nano-Fe3O4 Nanocomposite as a Lubricant Additive in Soybean Oil," *Lubrication Science* 36 (2024): 468–477.

59. M. A. Delgado, C. Valencia, M. C. Sánchez, J. M. Franco, and C. Gallegos, "Influence of Soap Concentration and Oil Viscosity on the Rheology and Microstructure of Lubricating Greases," *Industrial and Engineering Chemistry Research* 45 (2006): 1902–1910.

60. M. C. Sánchez, J. M. Franco, C. Valencia, C. Gallegos, F. Urquiola, and R. Urchegui, "Atomic Force Microscopy and Thermo-Rheological Characterisation of Lubricating Greases," *Tribology Letters* 41 (2011): 463–470.

61. J. E. Martín-Alfonso, C. Valencia, M. C. Sánchez, J. M. Franco, and C. Gallegos, "Development of New Lubricating Grease Formulations Using Recycled LDPE as Rheology Modifier Additive," *European Polymer Journal* 43 (2007): 139–149.

62. N. Acar, J. M. Franco, and E. Kuhn, "On the Shear-Induced Structural Degradation of Lubricating Greases and Associated Activation

Energy: An Experimental Rheological Study," *Tribology International* 144 (2020): 106105.

63. M. A. Delgado, E. Cortés-Triviño, C. Valencia, and J. M. Franco, "Tribological Study of Epoxide-Functionalized Alkali Lignin-Based Gel-Like Biogreases," *Tribology International* 146 (2020): 106231.

64. S. O. Ilyin, S. N. Gorbacheva, and A. Y. Yadykova, "Rheology and Tribology of Nanocellulose-Based Biodegradable Greases: Wear and Friction Protection Mechanisms of Cellulose Microfibrils," *Tribology International* 178 (2023): 108080.

Supporting Information

Additional supporting information can be found online in the Supporting Information section.